

Doppler Evaluation of Hemodynamic Changes in Uterine Blood Flow

G. Urban, H. Valensise, E. Ferrazzi, P. Beretta, P. Tortoli, L. Bonsignore, S. Ricci, P. Vergani, P. Patrizio and M. J. Paidas

INTRODUCTION

The main uterine artery and its branches are derivatives of the hypogastric artery. At the level of the internal cervical os, the uterine artery bifurcates into the descending (cervical) and ascending (to the body) branches. At the uterotubal junction, the ascending branch turns laterally and upward toward the ovary where it establishes anastomoses with the ovarian artery, forming an arterial arcade that provides perfusion to the upper aspect of the uterine corpus (see Chapter 22). Blood flow takes a linear course in the hypogastric artery, then turns in a serpentine course in the uterine artery, and finally regains a linear course throughout the gestation, as the uterus gradually increases in size.

Approximately eight to ten arcuate arteries originate from each uterine branch and envelope both the anterior and the posterior walls of the uterus for about one-third of the thickness of the myometrium¹. These arteries take a tortuous course and establish anastomoses with the corresponding arteries from the contralateral side in the midline of uterine myometrium (see Chapter 22).

The radial arteries arise from the arcuate arteries and are directed inward toward the uterine mucosa. The total number is undefined and most likely is dependent on parity and human biodiversity.

In the past, unsuccessful attempts were made to use conventional Doppler techniques to study uterine hemodynamic patterns to provide diagnostic clues for the management of postpartum hemorrhage (PPH). However, advances in signal acquisition and processing have facilitated precise and reproducible analyses of velocity profile patterns and other variables such as wall distension and shear rates at specific sites of the uterine circulation.

Several studies have shown a progressive decline in impedance in all compartments of the uterine circulation, from the main arteries to the spiral arteries, as pregnancy advances²⁻⁴. The impedance of the spiral arteries decreases and blood flow velocities increase between the 5th and 7th weeks of gestation. During that period, the hemodynamic status of the uterine and

arcuate arteries remains unchanged; it is only after the 8th week of gestation that a decrease in impedance and an increase in absolute flow velocities are detectable. This delay between the changes in the spiral and uterine arteries may represent the magnitude of the increase of placental volume and spiral arterial involvement, both of which are needed to effect appropriate and supportive uterine hemodynamics⁵.

INTRAPARTUM DOPPLER VELOCIMETRY

Fleischer *et al.*⁶ assessed 12 normal parturients throughout labor with a continuous wave Doppler unit to assess intrapartum changes in uterine and umbilical artery waveforms during labor. Each patient served as her own control. No significant changes were noted in umbilical artery systolic/diastolic (S/D) ratios before, during or after a uterine contraction in the latent phase of labor and with intact membranes, as well as in the active phase after rupture of membranes or during oxytocin stimulation. The uterine artery end-diastolic flow velocity fell progressively during uterine contractions, reaching 0 when the uterine pressure exceeded 35 mmHg. Despite intrauterine pressure of more than 60 mmHg, the diastolic notch did not appear. This study demonstrated that, at term, umbilical artery velocity waveforms do not change over a wide range of uterine pressures. Changes seen in uterine artery waveforms, on the other hand, suggested that the end-diastolic component is primarily determined by changes in the arcuate and spiral arteries, both of which are affected during uterine contractions.

MULTIGATE SPECTRAL DOPPLER ANALYSIS

In our studies, we used multigate spectral Doppler analysis (MSDA) to investigate blood flow. The MSDA overcomes the limitations related to the use of a single sample volume⁷⁻¹¹. With this method, 256 small sample volumes are aligned along an ultrasound scan line that intercepts the blood vessel, and the Doppler data from each sample volume are

independently analysed to produce a high-resolution flow profile. This non-standard method has been implemented in a system based on a proprietary electronic board connected to a commercial ultrasound machine (Aloka SSD1400) and a personal computer. The board, installed on a PCI slot of a host PC, samples the I/Q signals and processes the data in an on-board digital signal processor (DSP) to carry out the velocity profile. The profile is finally transferred in real-time to the PC to be displayed on the monitor.

The hypogastric, uterine and arcuate arteries were investigated in women in labor before epidural anesthesia, after at least 1 h postpartum, and in women before pregnancy. To our knowledge, no group of investigators had previously considered flow rates in terms of the capacity to sustain a life-threatening PPH.

This Doppler evaluation shows essentially how we define the bidimensional Doppler or '2-DD' quality

Doppler profile (QDP). Multi-sample volumes from multigate acquisitions along the scan line depict a bidimensional dynamic representation of the blood flow, where the horizontal axis is the depth and the longitudinal axis is the velocity. Actually, this is the best estimation in real-time of the blood flow throughout the vessels, showing an areal flow (cm^2/s) [from depth (cm) \times velocity (cm/s)]. Our experience shows that, during menses, areal flow through the arcuate artery is one-eighth (or perhaps one-tenth, depending on the anatomic variants) of the flow in the uterine artery, which is three-quarters of the flow in the hypogastric artery at the start of the menstrual cycle. This flow increases by one-third until ovulation (Figure 1) and remains constant until menstruation. By way of comparison, after conception and in early gestation, this flow increases until the end of the second trimester, after which it remains stable throughout

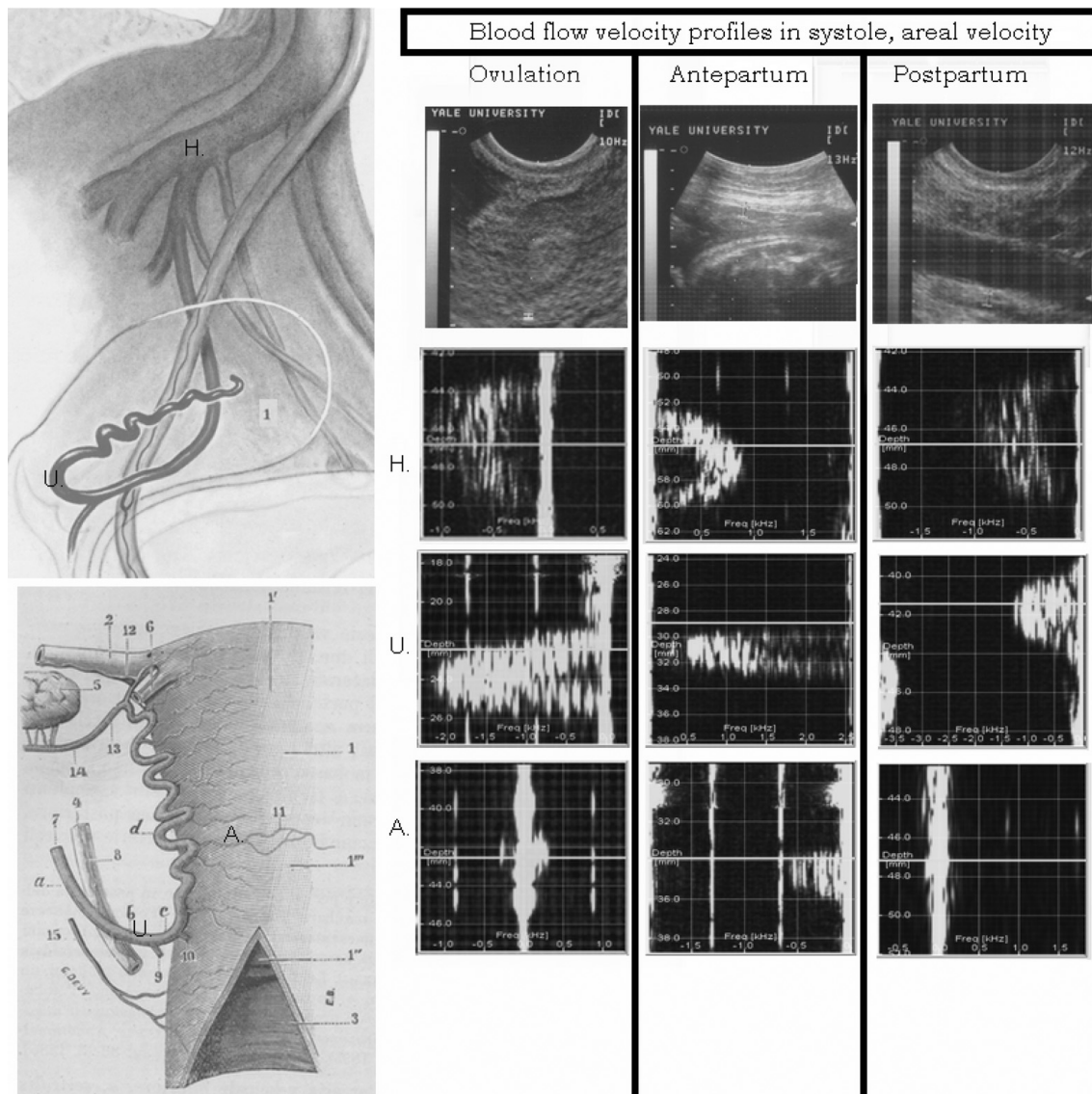


Figure 1 Multigate spectral Doppler analysis using GASP software for areal velocity in women at the ovulation phase of the normal menstrual cycle, in the antepartum phase of labor and at 1 h postpartum, respectively. In each column, the first image is the conventional bidimensional image of the area of interest during multigate acquisition, the following from top to bottom are hypogastric (H) artery velocity profile (areal flow), uterine (U) artery velocity profile (areal flow), and arcuate (A) artery velocity profile (areal flow). All images are frozen in systolic peak

labor, at which time the arcuate artery flow is one-fifth of the uterine, or almost double the flow before pregnancy. In the first and second stages of labor, this flow is markedly reduced, if not totally discontinued, by compressive action of the uterine contractions. During uterine contractions, the myometrial fibers also obliterate the flow in the radial arteries, reflecting the fact that they are tributaries of the arcuate arteries (see above), wherein flow stops until the end of contraction and then rises to reach a steady-state flow until the next contraction ensues. During each contraction, the placental lacunar space is compressed, thus pumping the blood to the fetal circulation throughout the umbilical vein. The compression of the radial arteries during each contraction acts as a valvular mechanism, avoiding reverse flow in the uterine circulation while, at the same time, directing the flow to the fetus. After delivery of the placenta, the resistance in the radial and spiral arteries decreases abruptly, being close to '0'. *As a consequence, there is an open flow of blood in the uterine cavity, which is contained by the compression caused by the prolonged uterine contractions. At this stage, the arcuate and radial flow is almost absent. The absence of flow through the radial and spiral arteries facilitates the clotting mechanism in the endometrial bed.*

Inefficiency of uterine contractions for whatever reason is an important risk factor for PPH. Likewise, an increase in the areal flow of the arcuate arteries, i.e. higher than one-fifth of the flow in the uterine arteries, is also a potential risk for PPH. The differences of areal flow between the hypogastric, uterine and arcuate arteries, in various physiologic conditions, including postpartum, are shown in Figure 1.

DIAGNOSTIC APPLICATION

After 10 years of our experimental work, the ultrasound industry has integrated this new Doppler signal processing made on MyLab from ESAOTE® (Florence, Italy) in a portable ultrasound machine. The velocity profile has been synthesized in a quality Doppler profile (QDP) function; this tool has the option DIR (direction) to indicate the mean interpolation of velocity profile in real time.

QDP is brand new technology developed by Esaote in collaboration with the University of Florence. QDP technology enables the acquisition of the signals of a large number of sample volumes placed across one or more blood flows. These sample volumes show the frequency content of each one of the related signals.

Studying the DIR shape of uterine artery immediately after delivery, we described the morphology of the uterine flow profile, comparing it with the postpartum quantity of blood loss.

Study design

We enrolled 236 consecutive women in labor. Within 15 min of placental delivery, both uterine arteries were investigated with approximately 60° of incidence using the QDP tool with the DIR activated at a

distance of twice the vessel diameter. After acquisition, the frame was frozen at the systolic peak in both arteries and the profile shape shown with DIR. Using the turbulence index (TI) classification, both arteries

Table 1 Data on 236 women in labor evaluated between October 7 2010 and December 27 2010. Data are expressed as numbers and percentages unless otherwise stated

	n	%
<i>Parity</i>		
0	135	57.2
1	81	34.3
2	16	6.8
3	2	0.8
4	2	0.8
Gestational week	39 ± 1.4	
Previous cesarean section	9	3.8
Maternal age (years)	31.5 ± 1.5	
<i>Induction</i>		
Vaginal dinoprostone 2 mg	57	24.2
1 dose	25	10.6
2 doses	21	8.9
3 doses	8	3.4
4 doses	3	1.3
Oxytocin	83	35.2
Dilating time at the admission (min)	120 ± 90	
Expulsive time (min)	28.5 ± 21.2	
Birth weight (g)	3360 ± 423	
Blood loss (ml)	200 ± 233	
PPH (blood loss >1000 ml)	17	7
Bakri balloon insertion	7	3

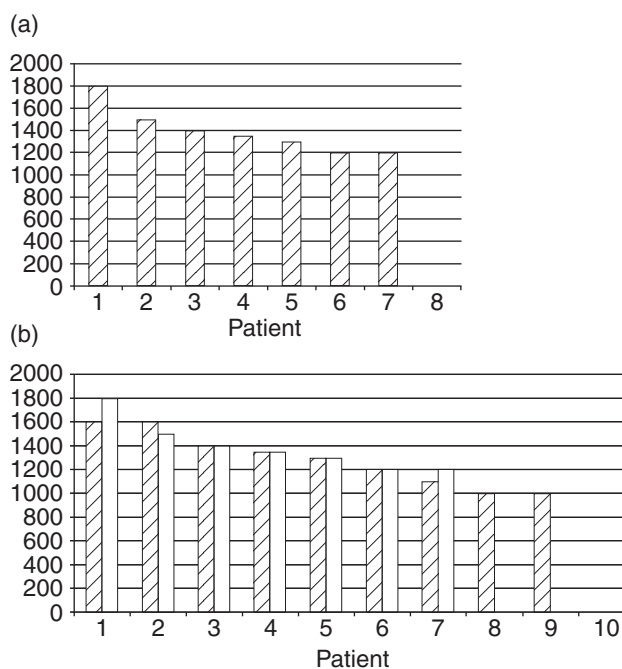


Figure 2 (a) Graph of blood losses (ml) of seven Bakri balloon patients. (b) Graph blood losses (ml) in PPH patients with Bakri balloon insertion (hollow bars) and without insertion (hatched bars)

where assigned a value between 0 and 3 (0 with maximum convexity and 3 maximum turbulence). Parity, gestational age, maternal age, previous cesarean section, dosage and mode of induction, labor duration, operative or spontaneous vaginal delivery, and blood loss, were recorded and analysed using non-parametric Spearman r^s .

Results

We evaluated 236 women in labor between October 7 2010 and December 27 2010, at a mean gestational age of 39 weeks. Of these, 24% underwent induction of labor, 87% had vaginal delivery and 12% vacuum operative delivery. Birth weight ranged between 1790 and 4330 g. Postpartum blood losses ranged between 50 and 1800 ml. In 17 cases, patients were determined

to have PPH (blood loss of 1000 ml or more); seven cases required Bakri balloon insertion (Figure 2).

When patients were divided into three classes by quantity of blood loss (<500 ml, between 500 and 1000 ml, and >1000 ml), we found an inverse correlation between the turbulence index (TI) and blood loss ($r^s -0.651$; $p < 0.0001$); the correlation was similar for birth weight ($r^s -0.156$; $p < 0.017$). In contrast, no correlation was present between induction and blood loss. Interestingly, in the seven cases of Bakri insertion the TI was 1 before insertion, whereas it became 3 after inflation of 250 ml.

CONCLUSIONS

We found a strict correlation between the TI and blood loss, in PPH and non-PPH, as well as before and

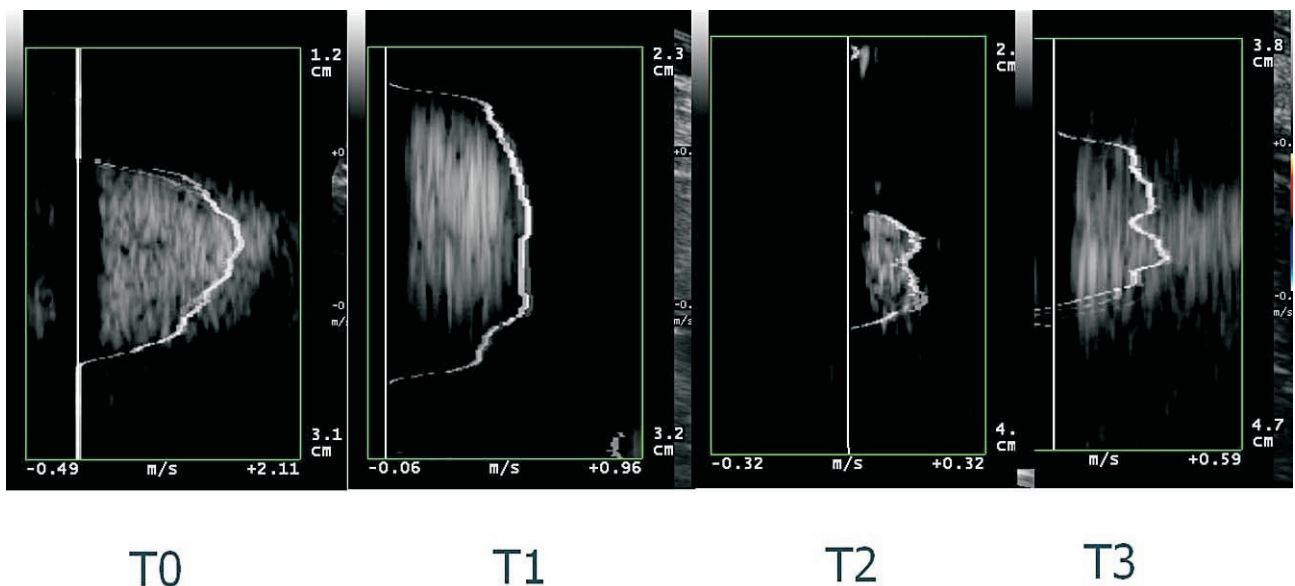


Figure 3 Quality Doppler profile (QDP) example of each profile in peak systolic in uterine artery at postpartum according to the turbulence index classification

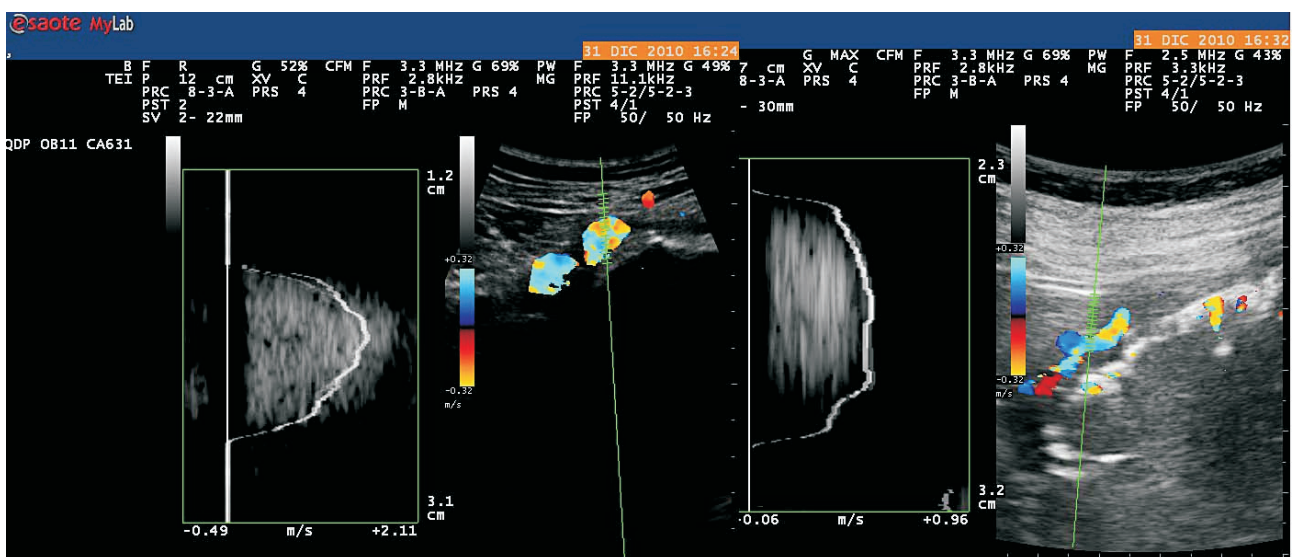


Figure 4 Sequence shows the mutation of flow profile from pseudolaminar flow during a PPH into the turbulent flow 8 min after the final of inflation of 250 ml of water into the Bakri balloon

after insertion of Bakri balloon, even if in a small series. Figure 3 shows examples of different classes of TI from 0 to 3. Figure 4 shows an example of the effect on the QDP of the inflation of Bakri balloon. The routine use of ultrasound in labor in our study was also useful in seven cases for contextual diagnosis of retained material individuation, as recently remarked in a retrospective study¹². The combination of portable ultrasound system and the integration of QDP is now a new diagnostic tool to monitor bleeding and risks for PPH.

ACKNOWLEDGMENTS

Our thanks go to Dr Lorenzo Battiato and Giorgio Pardi Foundation for non-profit funding support and to Esaote Research and Development for their industrial support.

References

1. Ramsey EM, Donner MW. Placental Vasculature and Circulation. Stuttgart: Georg Thieme, 1980
2. Jurkovic D, Januniaux E, Kurjak A, et al. Transvaginal color Doppler assessment of the uteroplacental circulation in early pregnancy. *Obstet Gynecol* 1991;77:365–9
3. Jauniaux E, Jurkovic D, Campbell S, et al. Doppler ultrasonographic features of the developing placental circulation; correlation with anatomic findings. *Am J Obstet Gynecol* 1992;166:585–7
4. Arduini D, Rizzo G, Romanini C. Doppler Ultrasonography in early pregnancy does not predict adverse pregnancy outcome. *Ultrasound Obstet Gynecol* 1991;1:180–5
5. Makikallio K, Tekay A, Jouppila P. Uteroplacental hemodynamics during early human pregnancy: a longitudinal study. *Gynecol Obstet Invest* 2004;58:49–54
6. Fleischer A, Anyagebunam A, Schulman H, et al. Uterine and umbilical artery velocimetry during normal labor. *Am J Obstet Gynecol* 1987;157:40–3
7. Bambi G, Morganti T, Ricci S, et al. A novel ultrasound instrument for investigation of arterial mechanics. *Ultrasonics* 2004;42:731–7
8. Tortoli P, Guidi G, Berti P, Guidi F, Righi D. An FFT-based flow profiler for high-resolution in vivo investigations. *Ultrasound Med Biol* 1997;23:899–910
9. Tortoli P, Michelassi V, Bambi G, Guidi F, Righi D. Interaction between secondary velocities, flow pulsation and vessel morphology in the common carotid artery. *Ultrasound Med Biol* 2003;29:407–15
10. Urban G, Paidas MJ, Bambi G, et al. Multigate spectral Doppler analysis, new application in maternal-foetal science. *Ultrasound Obstet Gynecol* 2004;24:217–8
11. Morganti T, Ricci S, Vittone F, Palombo C, Tortoli P. Clinical validation of common carotid artery wall distension assessment based on multigate Doppler processing. *Ultrasound Med Biol* 2005;31:937–45
12. Lousquy R, Morel O, Soyer P, Malartic C, Gayat E, Barranger E. Routine use of abdominopelvic ultrasonography in severe postpartum hemorrhage: retrospective evaluation in 125 patients. *Am J Obstet Gynecol* 2011;204:232